JOURNAL OF MORPHOLOGY 273:211–225 (2012)

Spinal Cord Regeneration in a Tail Autotomizing Urodele

Ellen M. Dawley,* Shoji O. Samson, Kenton T. Woodard, and Kathryn A. Matthias

Department of Biology, Ursinus College, Collegeville, Pennsylvania 19426

ABSTRACT Adult urodele amphibians possess extensive regenerative abilities, including lens, jaws, limbs, and tails. In this study, we examined the cellular events and time course of spinal cord regeneration in a species, *Plethodon cinereus*, that has the ability to autotomize its tail as an antipredator strategy. We propose that this species may have enhanced regenerative abilities as further coadaptations with this antipredator strategy. We examined the expression of nestin, vimentin, and glial fibrillary acidic protein (GFAP) after autotomy as markers of neural precursor cells and astroglia; we also traced the appearance of new neurons using 5-bromo-2′-deoxyuridine/neuronal nuclei (BrdU/NeuN) double labeling. As expected, the regenerating ependymal tube was a major source of new neurons; however, the spinal cord cranial to the plane of autotomy showed significant mitotic activity, more extensive than what is reported for other urodeles that cannot autotomize their tails. In addition, this species shows upregulation of nestin, vimentin, and GFAP within days after tail autotomy; further, this expression is upregulated within the spinal cord cranial to the plane of autotomy, not just within the extending ependymal tube, as reported in other urodeles. We suggest that enhanced survival of the spinal cord cranial to autotomy allows this portion to participate in the enhanced recovery and regeneration of the spinal cord. J. Morphol. 273:211–225, 2012.

KEY WORDS: spinal cord; regeneration; tail; autotomy

INTRODUCTION

Adult urodele amphibians possess extensive abilities to regenerate complex structures, including lens, jaws, limbs, and tails (Chernoff et al., 2003; Del Rio-Tsonis and Tsonis, 2003; Nye et al., 2003). In the case of tail regeneration, muscles, vertebral column, and spinal cord regenerate, which is perhaps linked to the unlimited growth potential of their tails (Holder and Clarke, 1988; Benraiss et al., 1999). In this study, we examined the cellular events and time course of spinal cord regeneration in a urodele species, *Plethodon cinereus*, that has the ability to autotomize its tail as an antipredator strategy. Many salamanders in the family Plethodontidae possess a unique suite of adaptations that allow them to detach their tails (autotomy; Wake and Dresner, 1967) and facilitate regeneration. When autotomized versus amputated tail wound healing and regeneration were compared using *P. cinereus*, all steps in these processes began and were completed sooner in autotomized tails (Dinsmore, 1977). All other spinal cord regeneration studies in urodeles have been done on species that cannot autotomize their tails; we expect that *P. cinereus* and other autotomizing species may have enhanced regenerative abilities as a coadaptation with this antipredator strategy.

The frequent presence of mitotic figures in the regenerating ependymal tube (Egar and Sinder, 1972; Iten and Bryant, 1976; Dinsmore, 1977; Chernoff et al., 2003) and studies using 5-bromo-2′-deoxyuridine (BrdU) to label mitotic cells in the ependymal tube (Benraiss et al., 1999; Ferretti et al., 2003) provide strong evidence that the radial ependymal cells forming the caudally extending ependymal tube divide and are the source of new neurons. Thus, the ependymal cells lining the central canal of urodele spinal cords appear to retain characteristics of embryonic radial glial cells. In addition, neurons from the intact spinal cord stump can migrate into the regenerate (Zhang et al., 2003). We predict that regeneration may commence more rapidly in *P. cinereus* than in these other urodele species because wound healing and cleanup commence more rapidly. We used double label experiments with anti-BrdU and anti-neuronal nuclei (NeuN, a reliable immunocytochemical marker for postmitotic neurons, Mullen et al., 1992) to locate and trace the appearance of new cells and their progression to expression of NeuN as postmitotic neurons.

Because adult neural stem cells are thought to express or re-express intermediate filament

Shoji O. Samson is currently at Touro College of Osteopathic Medicine, New York, NY.

Kenton T. Woodard is currently at University of North Carolina, School of Medicine, Chapel Hill, NC.

Kathryn A. Matthias is currently at Department of Microbiology and Immunology, Drexel University, Philadelphia, PA.

Contract grant sponsor: Ursinus College, HHMI, and Merck.

*Correspondence to: Ellen M. Dawley, Department of Biology, Ursinus College, Collegeville, PA 19426.
E-mail: edawley@ursinus.edu

Received 26 December 2010; Revised 29 July 2011;
Accepted 12 August 2011

Published online 28 September 2011 in
Wiley Online Library (wileyonlinelibrary.com)
DOI: 10.1002/jmor.11019

proteins in a pattern that mirrors embryonic development (Hockfield and McKay, 1985; Fredericksen and McKay, 1988; Wiese et al., 2004; Kempermann, 2006), an approach to documenting precursor cell activity is to characterize the timing and location of different intermediate filament proteins. We examined the expression of nestin, vimentin, and glial fibrillary acidic protein (GFAP) in *P. cinereus* intact and regenerating spinal cords at specific time points soon after induced tail autotomy. Nestin is abundant in early neuroepithelial and other embryonic and fetal cells; after differentiation into neural, pancreatic or hepatic cell lineages, nestin is downregulated, and, in the case of neurons, neurofilament proteins are upregulated, although the two proteins are briefly coexpressed. Nestin also is expressed in radial glia throughout the development of the central nervous system (CNS) (Hockfield and McKay, 1985). Nestin positive cells are found in some adult mammalian neural tissues that are radial glial-like, meaning that they are capable of cell division, differentiation, and migration (Doetsch et al., 1999; Doyle et al., 2001; Fukuda et al., 2003) and nestin is re-expressed after injury (Namiki and Tator, 1999). Thus, nestin is often used as a neural precursor cell marker (Kempermann, 2006).

Vimentin, another intermediate filament protein, also is expressed in neuroepithelial cells before differentiation (Tapscott et al., 1981; Cochard and Paulin, 1984; Fredericksen and McKay, 1988), concurrently (Fredericksen and McKay, 1988; Tohyama et al., 1992) and possibly after (Doyle et al., 2001) nestin expression. Similar to nestin, following early embryonic development, vimentin is for a period coexpressed with neurofilament proteins in some young neurons, but then disappears in mature neurons (Cochard and Paulin, 1984). During development, vimentin also is expressed in radial glial fibers (Shaw et al., 1981; Tapscott et al., 1981; Tohyama et al., 1992) and immature astrocytes (Eng and Lee, 1995); in adults, vimentin is expressed in ependymal cell bodies, tanycyte processes (Shaw et al., 1981), and Bergmann glial processes (Shaw et al., 1981). It is expressed in high levels in all portions of adult olfactory neurons (Schwob et al., 1986); because olfactory receptor neurons rarely express neurofilament proteins, Schwob et al. (1986) interpreted this expression pattern to be a failure of olfactory receptor neurons to switch to an adult intermediate protein composition and a retention of a more juvenile stage.

The third intermediate filament protein of interest is GFAP, which is expressed in radial glia at later developmental stages than that of the earliest expressions of nestin and vimentin (Tohyama et al., 1992). GFAP-positive processes of astrocytes are prevalent throughout the entire adult brain (Shaw et al., 1981; Tapscott et al., 1981), and some of these processes are also vimentin positive, although GFAP has a much wider distribution than vimentin, mostly replacing vimentin as astrocytes mature (Dahl, 1981; Eng and Lee, 1995). GFAP is traditionally said to be found in adult cells of the astroglial lineage, including differentiated astrocytes (Eng and Lee, 1995) and radial glia-like cells in the same adult mammalian neurogenic zones mentioned above that express nestin (Doetsch et al., 1997; Seri et al., 2001).

In the nonautotomizing urodele species that have been studied (*Ambystoma mexicanum*, *Pleurodeles waltl*, *Nothophthalmus viridescens*, *Triturus carnifex*, and *Salamandra salamandra*), GFAP expression was most often examined, vimentin expression was examined in many, and nestin expression was examined rarely. Unfortunately, no clear trends of expression of intermediate filament proteins in urodeles have emerged. For example, in most species, GFAP is most strongly expressed in the radiating and branching processes of radial glia, although some reported light expression in ependymal cell bodies, and one species appears to express no GFAP (Zamora and Mutin, 1988; Naujoks-Manteuffel and Roth, 1989; Holder et al., 1990; Arsanto et al., 1992; O'Hara et al., 1992; Lazzari et al., 1997; Walder et al., 2003). After tail amputation, GFAP immunoreactivity was reported either to have disappeared for several weeks in the regenerate (O'Hara et al., 1992) or to be upregulated in ependymal cells and their processes after a brief period when expression is lost (Walder et al., 2003). We have sought to present a coherent picture of the expression of these intermediate filament proteins in *P. cinereus* for comparison to other urodeles and to other vertebrates; we expect that the regenerating ependymal tube will express nestin first, then vimentin, and, finally, GFAP.

MATERIALS AND METHODS

P. cinereus, completely terrestrial salamanders, were collected in forests in Montgomery County, PA, and returned to specific collection sites after experimentation. They were housed at Ursinus College, where all work was carried out between 2005 and 2010, singly or in pairs in containers with moist filter paper at 14°C in a 12-h dark/12-h light cycle and fed *Drosophila* ad libitum. A salamander was forced to autotomize the distal 10 cm of the tail tip when the tail was gripped with forceps at 10 cm and the animal twisted its body to escape. After a specific number of days, the tail stump was reamputated and the entire tail processed as described below. The Ursinus College IACUC approved all care and procedures (Protocol #2004-2C).

For general morphology, tail stumps ($n = 5$) were immersion fixed overnight in 2.5% glutaraldehyde in 0.1 mol l^{-1} phosphate buffer (PB), rinsed in PB, and decalcified in 0.1 mol l^{-1} ethylenediaminetetraacetic acid for 4 days. They were postfixed in 2% osmium tetroxide for 1 h, brought through a series of ethanols of increasing concentration, and embedded in Poly/Bed-Araldite (Electron Microscopy Services). Tails were cut transversely with glass knives on a rotary microtome at a thickness of 0.5 μm. Sections were mounted on a slide and stained with 1% toluidine blue.

We used BrdU to birth date ependymal cells. Salamanders were injected intraperitoneally five times, at 1 h intervals, with

BrdU (0.050 mg/g body weight; Sigma) 3 or 6 days after tail autotomy. Tail stumps were reamputated 1 day to 3 weeks after BrdU injection (n = 10–20 for each time point). Controls consisted of salamanders (n = 5) injected with BrdU without tail autotomy; the distal one-third of tails then were amputated 1 day after BrdU injection.

For all immunohistological procedures, tail stumps were immersion fixed overnight in 4% paraformaldehyde, rinsed in PB, and cryoprotected overnight in 30% sucrose. Tail stumps were frozen sectioned at 10–12 μm, and each section was collected on Fisher Superfrost slides or slides treated with Biobond (Electron Microscopy Services). A minimum of five slides, with 10–15 serial sections on each slide, were collected, which always resulted in sections that spanned from caudal-most regenerating tail into more cranial sections with intact spinal cord. Slides were dried overnight at 45°C and then stored in the freezer until further processing. When ready to proceed further, slides were first warmed for 1–2 h, rinsed in phosphate buffered saline (PBS), then brought through a series of ethanols (70, 95, 100, 95, and 70%) and back to PBS. To localize cells that incorporated BrdU, sections were incubated in 1 N HCl for 10 min at room temperature, then in 2 N HCl for 30 min at 37°C, and neutralized in 0.1 mol l^{-1} borate buffer (pH 8.5) for 5 min, followed by rinsing in PBS. After blocking (10% normal goat serum, 4% bovine serum albumin (BSA), 5% nonfat dry milk, 0.2% Triton X-100, and 0.0004% sodium azide in PBS) for 30 min, slides were incubated in a cocktail of primary antibodies (rat anti-BrdU diluted 1:100, Accurate Chemicals; mouse anti-NeuN diluted 1:250, Millipore) for 3 days at room temperature. After rinsing in BSA wash (4% BSA, 5% nonfat dry milk in PBS), slides were then incubated for 3 days at room temperature in a cocktail of secondary antibodies (Alexa Fluor 488 goat anti-rat and Alexa Fluor goat anti-mouse, both diluted 1:500; Invitrogen), followed by washes in BSA wash and PBS, and coverslipped with Fluoromount (Electron Microscopy Services). For nestin and vimentin double labeling, tail stumps were reamputated 2–21 days after autotomy (n = 10–20 for each time point). Nestin/vimentin controls (n = 6) were the distal one-third of tails without prior autotomy. A similar tissue and slide processing procedure was followed as for the BrdU/NeuN double labeling, minus the incubation with HCl and borate buffer, such that following the ethanol series, slides were blocked for 20 min and then incubated in primary antibodies (mouse antinestin, diluted 1:50, Millipore; rabbit antivimentin, 1 μg/ml, Abcam) for 1.5 h at room temperature. After rinsing in BSA wash, slides were incubated in secondary antibodies (Alexa Fluor 546 goat anti-mouse and Alexa Fluor 488 goat anti-rabbit, 1:500 dilution) for 1 h at room temperature, rinsed in PBS, incubated for 4.5 min in Hoechst (1:500 dilution; Sigma Chemicals), rinsed in PBS and then distilled water, and coverslipped in Fluoromount. For GFAP and NeuN double labeling, tail stumps were reamputated 3–66 days after autotomy (n = 5 for each time point) and controls (n = 5) were the distal one-third of tails without prior autotomy; a similar procedure was followed as for nestin/vimentin double labeling, but the primary antibodies consisted of rabbit anti-GFAP (diluted 1:500; Dako) and mouse anti-NeuN (diluted 1:500; Millipore), secondary antibodies were Alexa Fluor 488 goat anti-rabbit and Alexa Fluor 546 goat anti-mouse, followed by Hoeschst. Negative controls for all treatments consisted of the same steps described above, but the primary antibody was omitted; in all cases, omission of primary antibody resulted in no labeling. Sections were examined with a confocal microscope (Nikon Eclipse 80i) and photographed (Nikon D-Eclipse C1 camera).

RESULTS

Anatomy

The spinal cord in a normal (not regenerating) tail extended nearly to the tip of the tail and consisted of a double layer of cells surrounding an enlarged central canal without an obvious peripheral neuropil layer (Fig. 1A). Proceeding cranially, the number of cells within the gray matter gradually increased, particularly in the dorsal part of the cord, as did the thickness of the white matter and density of neuropil within the white matter (Fig. 1B–F). In addition, the diameter of the central canal decreased and the shape of the spinal cord changed when moving cranially; the spinal cord became progressively rounder (Fig. 1D), then rhomboidal in shape (Fig. 1E), and finally somewhat compressed dorsoventrally (Fig. 1F), and remained that shape throughout the rest of the tail. One day after tail autotomy, no portion of a spinal cord was visible in tissue at the distal-most tip of the tail stump, but within 50–75 μm cranially, a remnant of the spinal cord appeared, composed mostly of acellular material (Fig. 2A). Moving another 75 μm cranially, the spinal cord appeared intact. One week after tail autotomy, remnants of a damaged spinal cord were still likely to be present at the distal end of the tail (Fig. 2B), rather than a simple ependymal tube, and the spinal cord remnant became progressively more complete in a cranial direction (Fig. 2C,D). This spinal cord remnant was composed of an enlarged central canal surrounded by an ependymal layer and more peripheral round cell bodies, which were NeuN-ir (Fig. 12). More peripherally yet, the surrounding white matter was disrupted, clearly lacking the dense neuropil of a normal spinal cord (Fig. 1D–F). Two weeks after tail autotomy, a growing ependymal tube (Fig. 2E) was reliably found at the distal tail tip, 5 μm cranial to the blastema; continuing cranially, the ependymal tube gradually transitioned into an intact spinal cord in another 90 μm.

BrdU

Spinal cord sections sampled along the distal one-third of control salamanders rarely contained BrdU-immunoreactive cells. In experimental specimens injected with BrdU 3 days after tail autotomy, an ependymal tube had not yet formed and the distal end of the spinal cord showed extensive damage. However, even in the remaining damaged spinal cord, BrdU-ir cells were scattered along its length, mainly in the ependymal layer, from the distal-most recognizable end to as far proximally as was sectioned. Thus, sections that contained labeled cells ranged from a spinal cord remnant with few cells (Fig. 3A) to sections that appeared to be complete and undamaged (Fig. 3B). In one specimen, there was, on average, one BrdU-ir cell per 12-μm-thick section for 15 sections (185 μm), although in other specimens there were no BrdU-ir cells in the spinal cord at all. In specimens 4 days after BrdU injection (which makes it 7 days

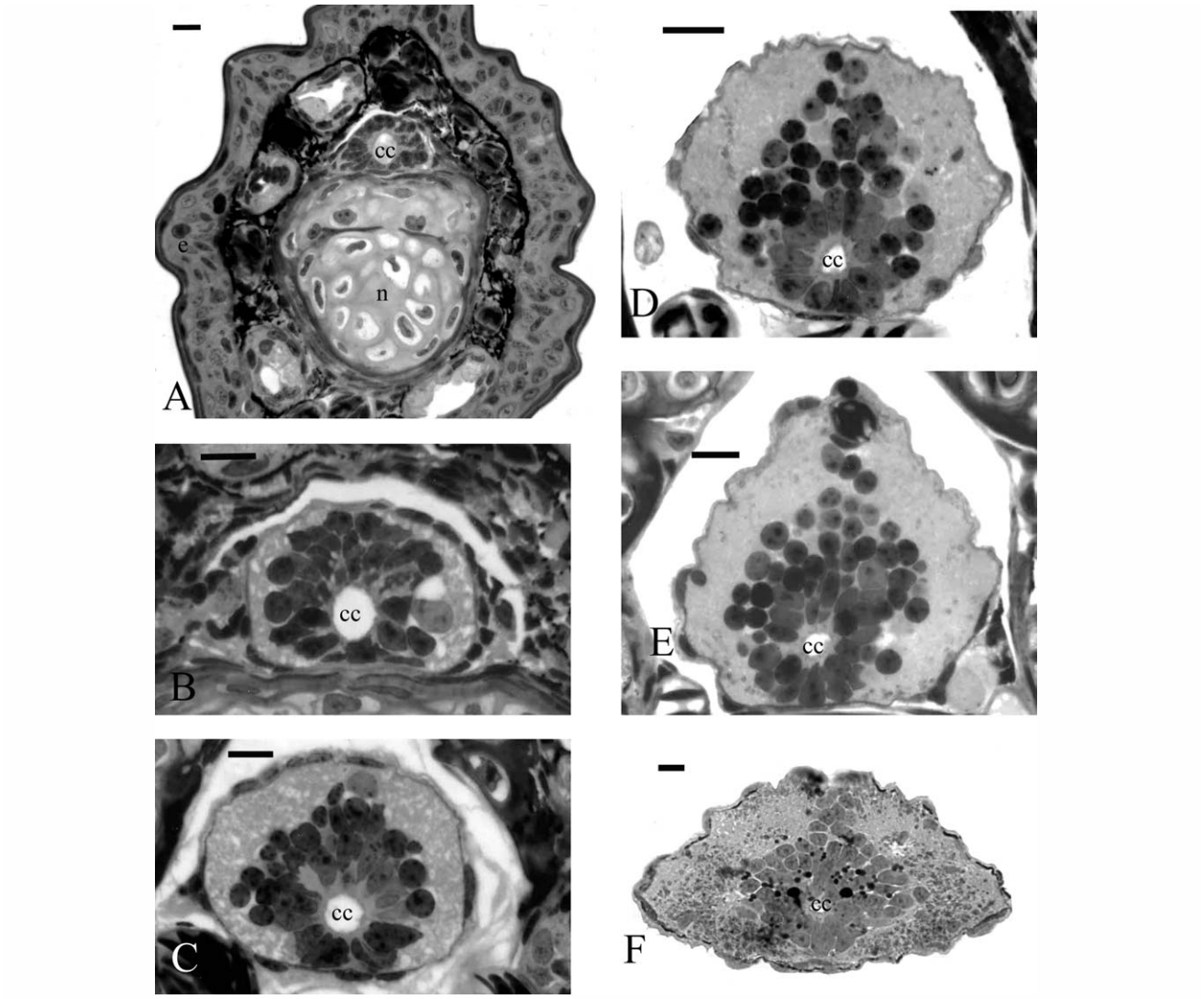

Fig. 1. Semithin sections of a normal (not regenerating) spinal cord stained with toluidine blue. **A**: The distal most tip of the spinal cord in place within the tail. **B–F**: Progressively more cranial sections, with F representing the spinal cord condition throughout the rest of the tail. cc, central canal; e, epidermis; and n, notochord; scale lines = 25 μm.

after autotomy), some BrdU-ir cells were peripheral to the ependymal layer.

BrdU injection at 6 days postautotomy was far more likely to label ependymal cells, and in some specimens nearly every ependymal cell in the ependymal tube was BrdU-ir (Fig. 4A), although in some specimens only some, often less than 1/2 of the ependymal tube cells, were BrdU-ir. In some cases, the ependymal layer continued to be labeled throughout the length of the sectioned regenerate (Fig. 4B–D), well into what seemed to be undamaged and unregenerated spinal cord (Fig. 4D); in this specimen, BrdU-ir ependymal cells were present along the entire 450-μm tail that was sectioned. In addition, some cells peripheral to the ependyma were BrdU-ir, and often these cells were dorsal to the central canal (Fig. 4C). This occurred in specimens 1 day after BrdU injection (Fig. 4) as well as all other treatments (2, 3, 4, 6, 8, 15, and 23 days post-BrdU injection), and BrdU-ir cells remained in the ependymal layer in all treatments. The distribution of BrdU-ir cells along the distal spinal cord varied among specimens, such that in some cases, there were more labeled ependymal cells in proximal sections than in the distal ependymal tube, yet in other cases, the more distal tip had many BrdU-ir cells even 15 days post-BrdU injection. However, the BrdU-ir in this specimen was mostly punctate (lesser in intensity) than in specimens with shorter periods of time between BrdU injection and reamputation, except in more proximal sections where the BrdU-ir was intense.

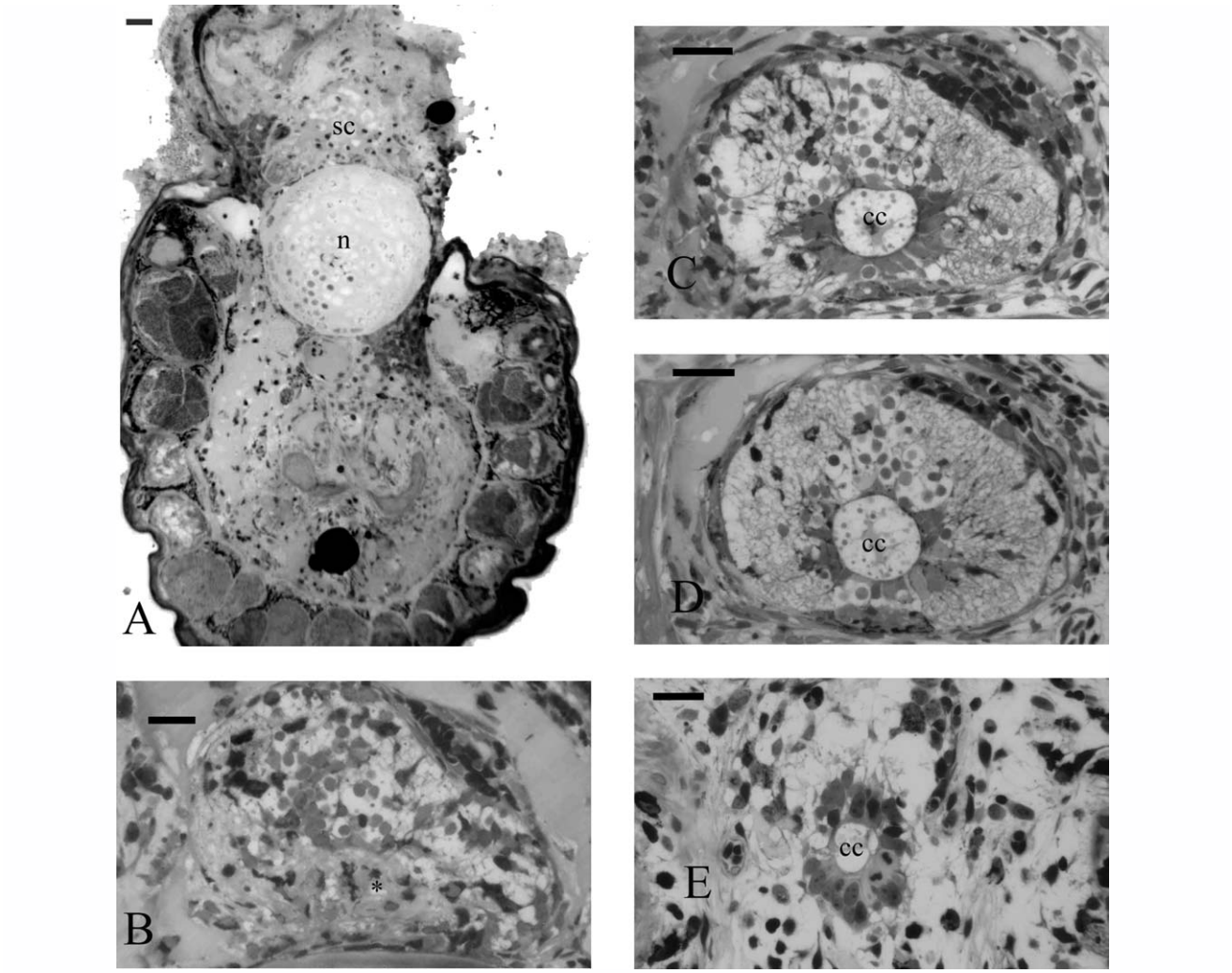

Fig. 2. Semithin sections of regenerating spinal cords stained with toluidine blue. **A**: Distal tip of entire regenerating tail 1 day after tail autotomy. The largely acellular area directly dorsal to the notochord (n) is the damaged spinal cord (sc). The skin is missing dorsally, but complete with skin glands ventrally. **B**: Distal end of spinal cord 1 week after tail autotomy; an asterisk marks where the central canal would be located. **C** and **D**: Same tail as B, at progressively more cranial positions; cc, central canal. **E**: Ependymal tube of regenerating spinal cord 2 weeks after tail autotomy; scale lines = 50 μm.

In specimens that had regenerated the longest (29 days postautotomy and 23 days post-BrdU injection), BrdU-ir cells were not present in the distal tip, but along a discreet length of the cord. For example, diffuse BrdU-ir was present distally at the stage when the spinal cord was already three layers thick, as the cord differentiated to contain neurons, until a level at which the spinal cord was nearly repopulated. This label was often, but not always, punctuate.

NeuN (and NeuN plus BrdU)

NeuN-ir cells colabeled with BrdU were present in the ependymal layer (Fig. 5A,B) and more peripherally (Fig. 5C,D) 1 day after BrdU injection, although this NeuN-ir was faint. However, not all BrdU-ir cells were also NeuN-ir. The intensity of the NeuN immunofluorescence varied within the same specimen and even within the same section, as did the size of the NeuN-ir cell bodies, although the intensity was always light within cells in the ependymal layer (Fig. 5D,E). In intact cranial sections, NeuN-ir was not detectable in ependymal cells, although the majority of periependymal cells were NeuN-ir (Fig. 5F). NeuN-ir also was variably present within the processes of neurons within the white matter (Fig. 6A,B), sometimes at a greater intensity than within the nucleus (Fig. 6B), although this was only true in more cranial sections with intact spinal cords. In specimens that had been regenerating for longer periods of time (33 days), it was possible to trace the orderly progression from elongate ependymal

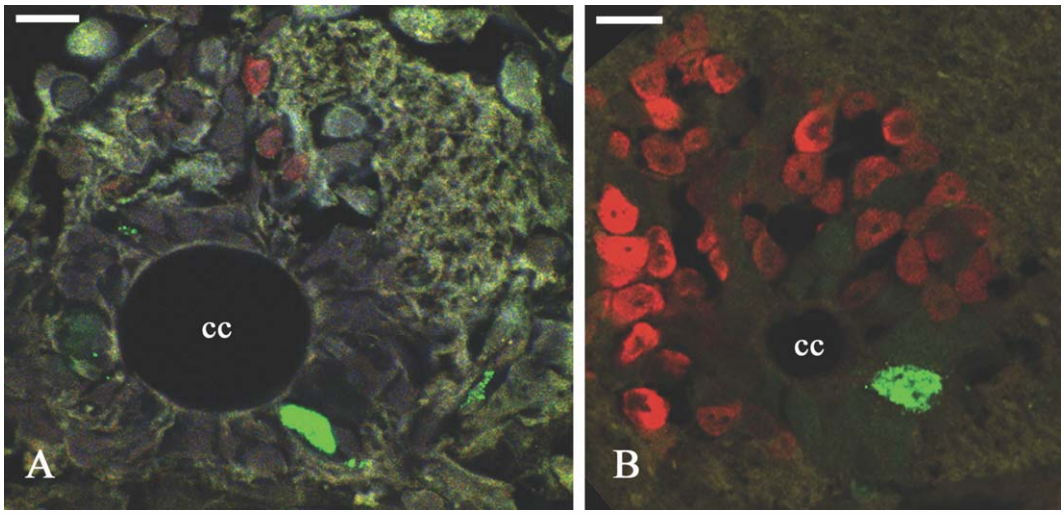

Fig. 3. Spinal cords injected with BrdU 3 days after tail autotomy, double labeled with anti-BrdU and anti-NeuN. **A**: Distal spinal cord remnant with enlarged central canal (cc). **B**: More cranial, more complete-looking spinal cord remnant without enlarged central canal. BrdU-immunoreactivity is green and NeuN-immunoreactivity is red; scale line = 20 μm.

cells to more peripheral, round, NeuN-ir cells (Fig. 5E,F). By 8 days after autotomy, when a growing ependymal tube was recognizable and remnants of the damaged cord were still present, NeuN-ir cells were located caudal to the ependymal tube (Fig. 7A) and even some distance from it (Fig. 7B). In slightly more proximal sections (Fig. 7C), NeuN-ir cells were adjacent to the ependymal layer. Even more proximally, NeuN-ir was also seen in the growing white matter as NeuN-ir cells continued to be added to the spinal cord (Fig. 7D). Sometimes, it was possible to identify a BrdU-ir cell that did not express NeuN and was oval in shape in both 3-day and 6-day BrdU injected salamanders. These could be macroglial cells rather than neurons. In comparison, NeuN-ir cells, which are neurons, are round.

Nestin/Vimentin

Nestin and vimentin immunoreactivity were considered together in double label experiments. Spinal cord sections sampled along the distal 1/3 of control salamanders only showed light vimentin/nestin immunoreactivity in very distal sections. Vimentin-ir cells were detected earlier than nestin-ir cells in the distal end of spinal cords, 2–4 days after tail autotomy; vimentin-ir ependymal cells were present in the distal damaged spinal cord as the ependymal tube had not yet formed (Fig. 8A). More proximally, yet still within the part of the spinal cord affected by the autotomy (not a complete complement of cells within the gray matter), there was abundant nestin immunoreactivity within the white matter of the spinal cord, often adjacent to cell bodies and often colocalized (yellow) with vimentin immunoreactivity, although this reactivity was not as intense as the nestin immunoreactivity (Fig. 8B–D). These were not radial fibers. Even more proximally, at the stage where the spinal cord appeared complete (possessed what looked like complete complement of cells), many cell bodies peripheral to the ependymal layer and within the gray matter were vimentin-ir, in addition to the nestin and vimentin white matter immunoreactivity (Fig. 9). Intense vimentin-ir radial fibers were present ventrolaterally (Fig. 9B). By 5 days postautotomy, nestin immunoreactivity could often be found along with vimentin immunoreactivity in ependymal cells (Fig. 10A; yellow is double label), although vimentin-ir was more intense in these cells. In more proximal sections (Fig. 10B), vimentin-ir was more intense than nestin-ir in the ependyma, but both were intense in the white matter. By 14 days postautotomy, the ependymal tube extending posteriorly was both nestin and vimentin immunoreactive, particularly within the developing white matter (Fig. 11A), but proximally cells in the peripheral gray matter expressed mainly vimentin (Fig. 11B) and little nestin, even though this portion of the spinal cord was still mitotically active (Fig. 11C). By 21 days postautotomy, some vimentin-ir cells were still evident in the peripheral gray matter. Spinal cord sections sampled along the distal one-third of control salamanders only showed light vimentin/nestin-immunoreactivity in very distal sections, similar to that pictured in Figure 11A.

GFAP

GFAP immunofluorescence in normal spinal cords was evident in the branching processes and the endfeet within the white matter (Fig. 12A),

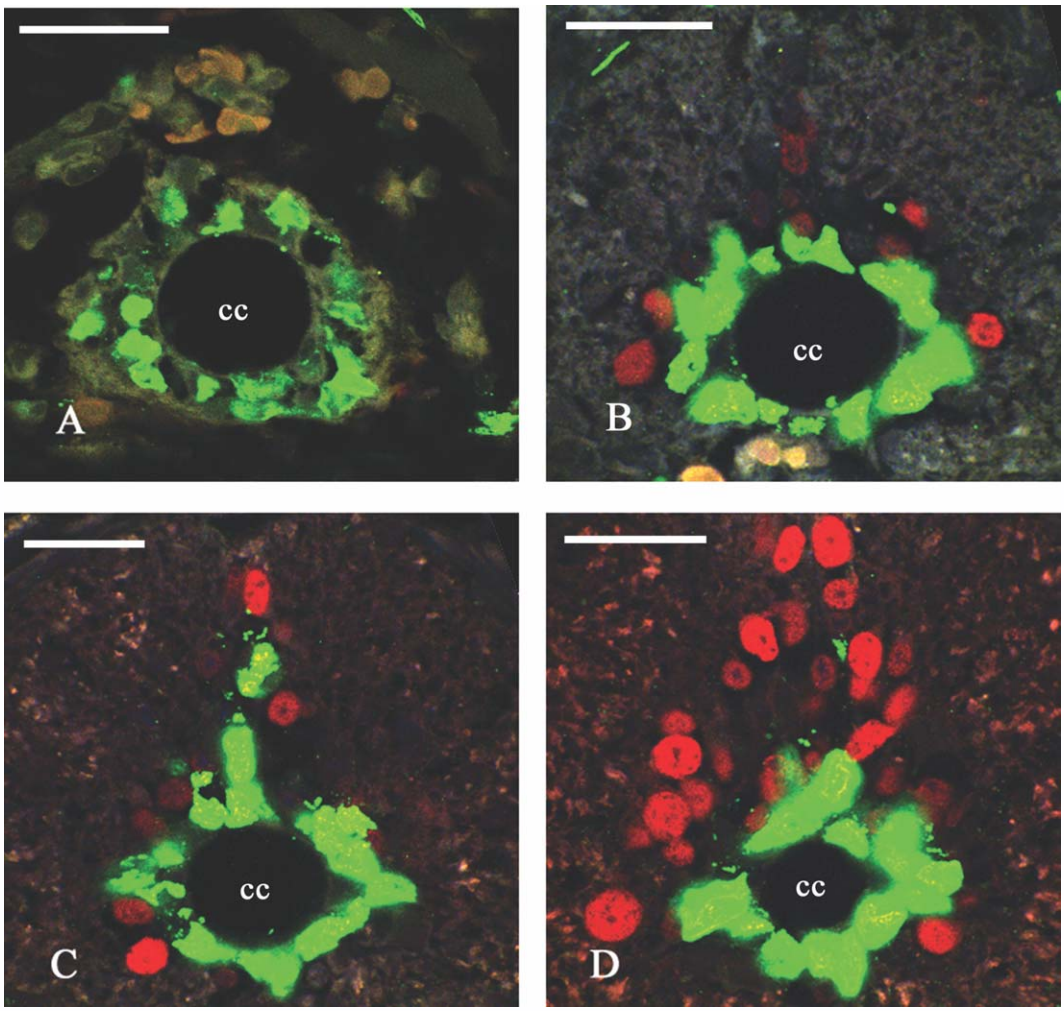

Fig. 4. Spinal cords injected with BrdU 6 days after tail autotomy, double labeled with anti-BrdU and anti-NeuN and reamputated 1 day after injection. **A**. Ependymal tube of regenerating spinal cord. **B–D**: Progressively more cranial, more complete-looking spinal cord remnants from the same animal. BrdU-immunoreactivity is green and NeuN-immunoreactivity is red; cc, central canal; scale line = 50 μm.

but not the cell bodies of cells in the ependymal layer, although more peripheral cell bodies within the gray matter occasionally seemed to be GFAP-ir. At the distal end of the regenerating spinal cord, white matter processes and endfeet remained GFAP-immunoreactive in the early stages of regeneration (e.g., 5 days postautotomy) even though damage was still evident and an ependymal tube had not yet emerged (Fig. 12B). Once an ependymal tube was recognizable distally (e.g., 2 weeks), GFAP-ir was intense in individual cell bodies, particularly those that appeared to be undergoing mitosis, and in many processes (Fig. 12C), and, more cranially, in cells of the ependymal layer (Fig. 12D,E) and the periependymal gray matter (Fig. 12E,F). In all days postautotomy, in the intact (possibly never regenerated) portion of the tail, long, thick fibers radiated from cells in the gray matter or lining the central canal and extended to the meningeal surface (Fig. 13); this label was always more intense than in normal, nonautotomized tails (Fig. 12A). In the oldest regenerating spinal cords (66 days after autotomization), at the distal end, GFAP immunofluorescence was intense in the cytoplasm of ependymal cells and in the growing white matter (Fig. 14A); GFAP immunofluorescence continued to be intensely expressed in the expanding white matter in more cranial sections (Fig. 14B,C).

DISCUSSION

BrdU/NeuN Results

Perhaps the most significant conclusion from these BrdU experiments in *P. cinereus* is that mitosis is not restricted to the growing ependymal tube, but also occurs in the distal end of the remaining spinal cord, which was at varying

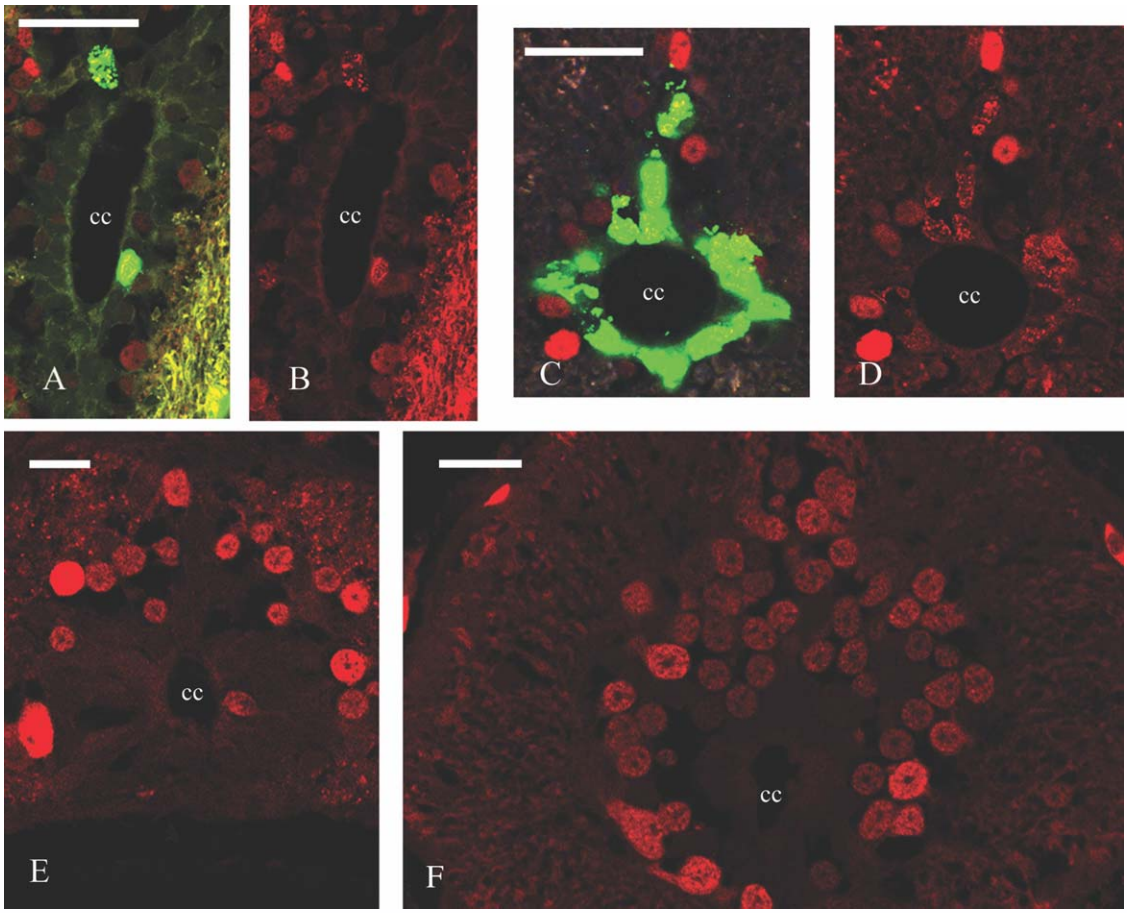

Fig. 5. Distribution and intensity of expression of NeuN-immunoreactivity. **A** and **B**: BrdU–NeuN double labeling 1 day after BrdU injection in a distal regenerate. **C** and **D**: BrdU–NeuN double labeling 1 day after BrdU injection in a more cranial section. **E**: NeuN-immunoreactivity in a 33-day regenerate. **F**: NeuN-immunoreactivity in a far cranial, intact section. BrdU-immunoreactivity is green and NeuN-immunoreactivity is red; cc, central canal; scale line = 50 μm.

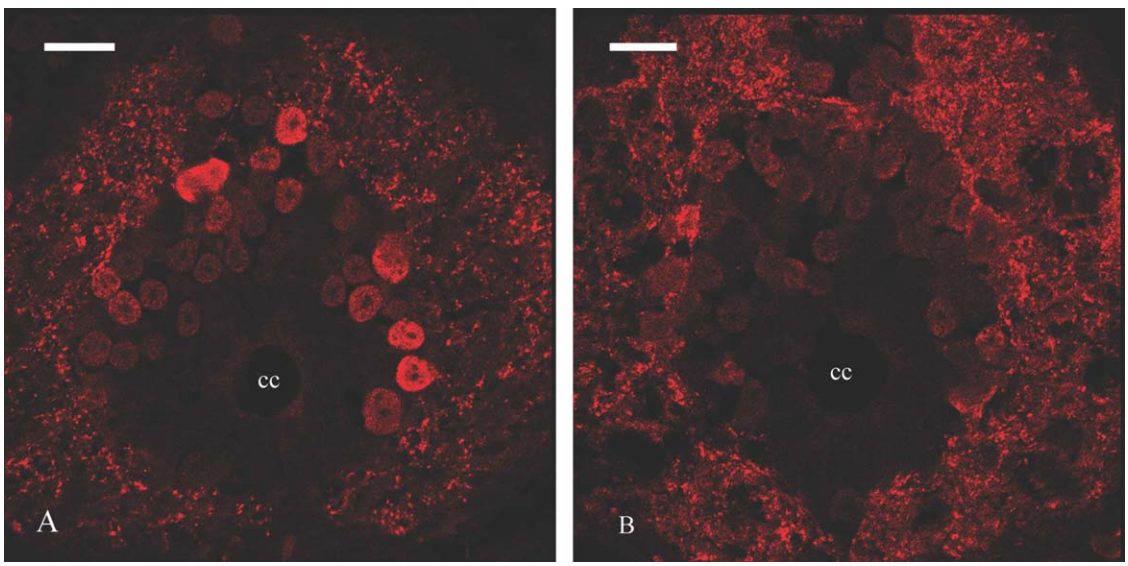

Fig. 6. Distribution and intensity of NeuN-immunoreactivity within the white matter. **A**: Light intensity with the white matter. **B**: Dark intensity within the white matter. NeuN-immunoreactivity is red; cc, central canal; scale line = 25 μm.

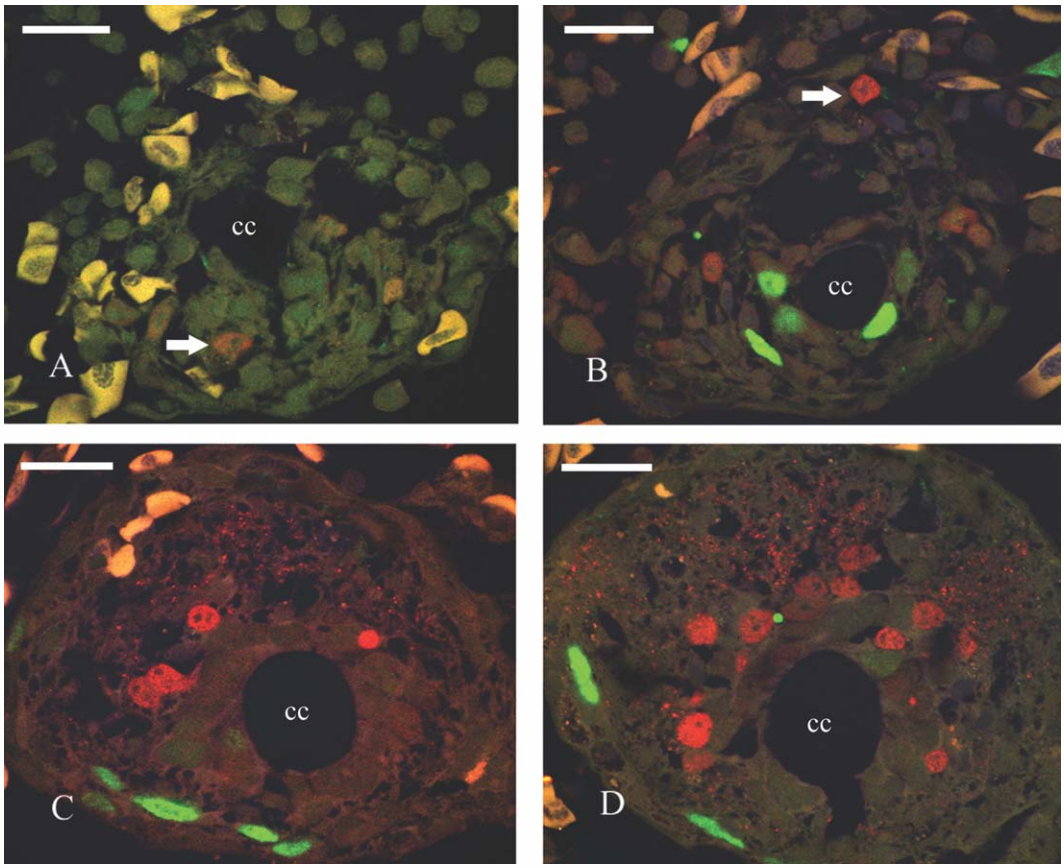

Fig. 7. Position of NeuN-ir cells in relation to the growing ependymal tube 8 days after autotomy. **A**: Caudal to the ependymal tube. **B**: At the level of the ependymal tube. **C** and **D**: Progressively more cranial to the ependymal tube. BrdU-immunoreactivity is green and NeuN-immunoreactivity is red; cc, central canal; scale line = 30 μm.

stages of damage, including sections that look completely undamaged and unregenerated. Thus, mitotic activity is upregulated even within the undamaged spinal cord. Sometimes these BrdU-ir cells are found peripheral to the ependyma as early as 1 day after BrdU injection, but they also remained in the ependyma even 23 days post-BrdU injection. In these latter, older regenerates, BrdU immunofluorescence was punctate most distally, perhaps indicating ependymal cells that had continued mitosis as the tube grew distally; however, some ependymal cells located more proximally in these long-term regenerates retained an intense BrdU immunofluorescence, perhaps indicating a cell that had not undergone any further mitosis and remained in place. In other urodele species that have been studied, all of which are incapable of tail autotomy, BrdU-ir cells were found in both the terminal vesicle and along the regenerating ependymal tube (Benraiss et al., 1997, 1999; Ferretti et al., 2003). However, these studies examined only the growing ependymal tube in 2- or 3-week regenerates and report the events of neither early regeneration nor the more proximal partial or completely intact spinal cord. A histological study of regeneration in *N. viridescens* showed mitosis in the growing ependymal tube as early as 5 days postamputation, although there was a substantial wound epidermis containing dead cells and tissue debris that was not cleared out until 10–15 days postamputation (Iten and Bryant, 1976). In our study, we document that mitosis is detectable in *P. cinereus* 3 days postautotomy within the ependymal tube and the undamaged spinal cord. More recently, Mchedlishvili et al. (2007) grafted green fluorescent protein-positive spinal cord portions onto recipient larval axolotl tails that had equivalent lengths of spinal cord removed. After a 7-day healing period, these tails were amputated and imaged over several days to reveal that a 500-μm region adjacent to the amputation plane generated the neural progenitors for regeneration. Similarly, 7 days after autotomy we identified a region of 400–500 μm cranial to the amputation plane that incorporated BrdU in *P. cinereus*. The wound healing of plethodontid salamanders results in tissues anterior to the myoseptum being only slightly disturbed, and even at

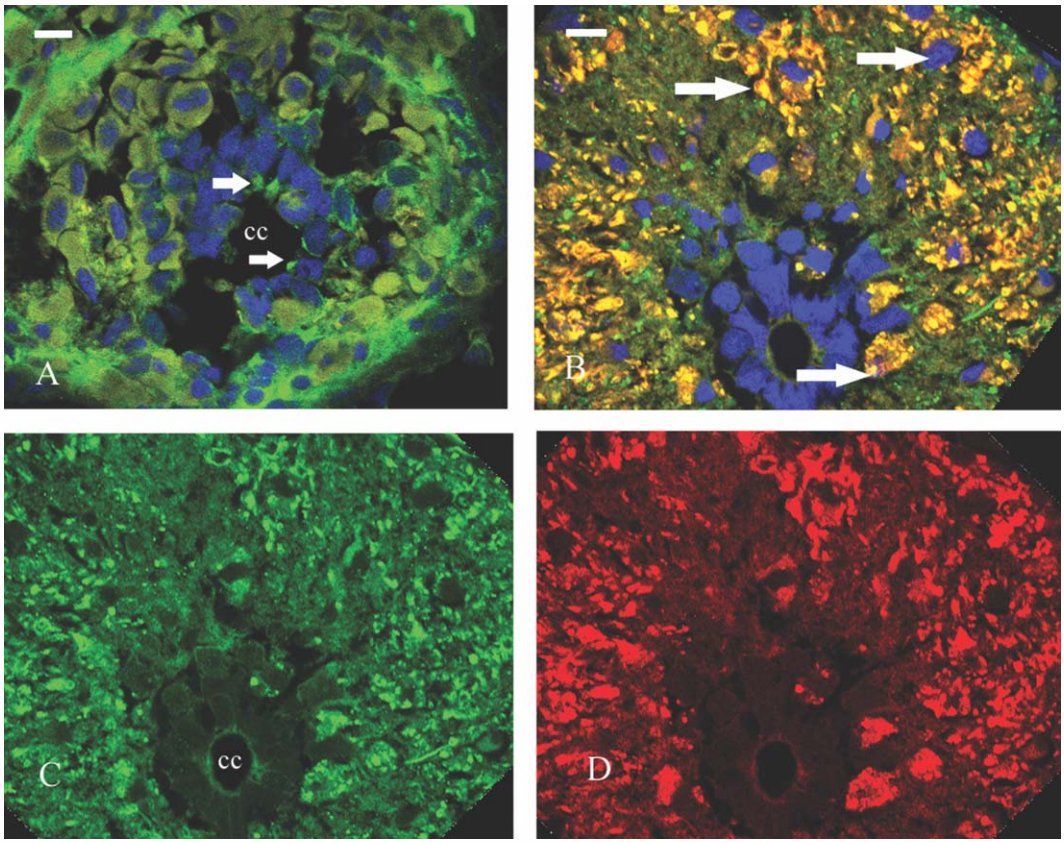

Fig. 8. Expression of nestin and vimentin in a spinal cord 2 days after autotomy. **A**: Distal section, close to the plane of autotomy; white arrows point to vimentin-immunoreactivity in the ependymal layer. **B–D**: More cranial section showing (B) combined nestin–vimentin immunoreactivity, white arrows point to large areas of nestin–vimentin colocalization adjacent to a nucleus, (C) vimentin-immunoreactivity alone, and (D) nestin-immunoreactivity alone. Vimentin-immunoreactivity is green; nestin-immunoreactivity is red; vimentin–nestin coexpression is yellow; and Hoescht nuclear label is blue; cc, central canal; scale line = 15 μm.

2-day postautotomy, the spinal cord one to two cells proximal to the stump surface are histologically undisturbed (Dinsmore, 1977). This adaptation may mean that the distal spinal cord that is proximal to the regenerating ependymal tube is more likely, or more quickly, to participate in the events of regeneration, as was seen in our study. Comparisons of BrdU incorporation in other spe-

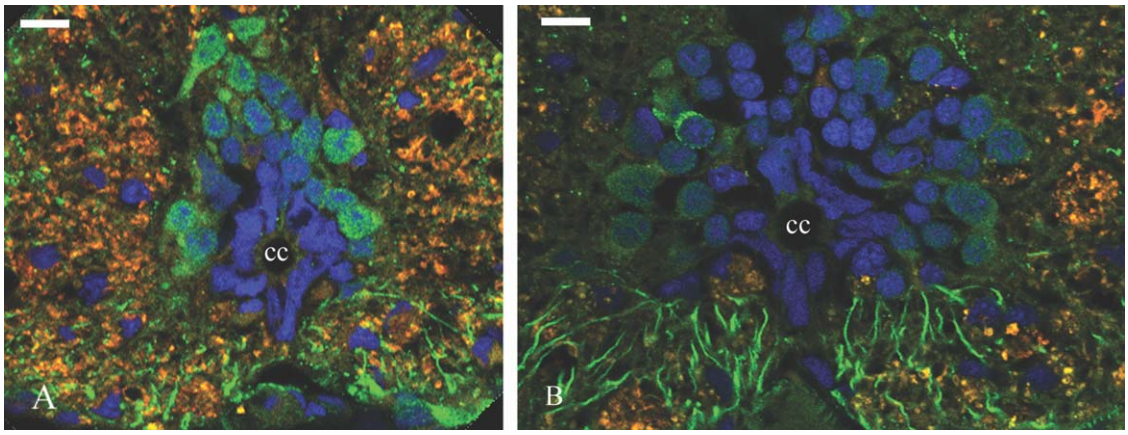

Fig. 9. Nestin and vimentin-immunoreactivity in a cranial, undamaged portion of the spinal cord 4 days after autotomy. **A**: Strong vimentin-ir in cell bodies. **B**: Strong vimentin-ir radial fibers. Vimentin-immunoreactivity is green; nestin-immunoreactivity is red; vimentin–nestin coexpression is yellow; and Hoescht nuclear label is blue; cc, central canal; scale line = 15 μm.

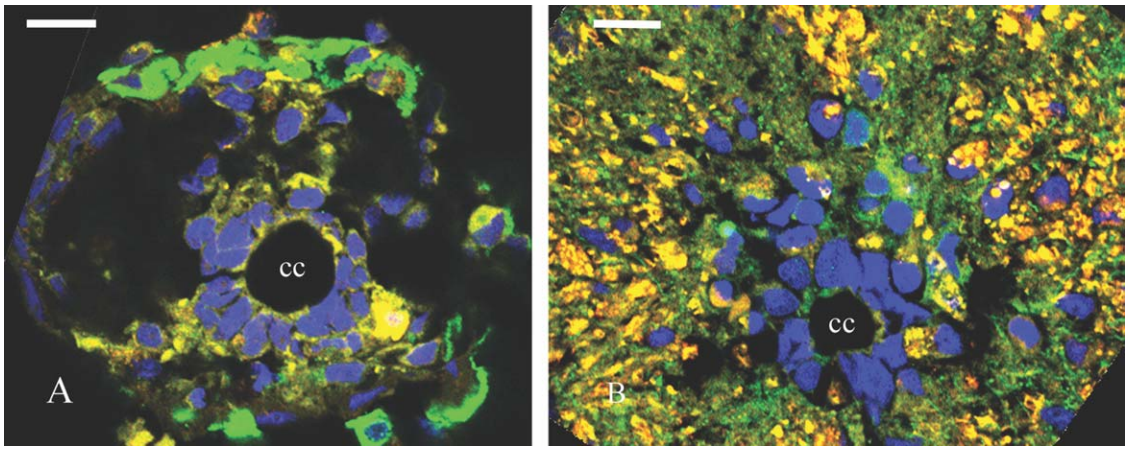

Fig. 10. Expression of nestin and vimentin in a spinal cord 5 days after autotomy. **A**: Distal section, close to the plane of autotomy. **B**: More cranial section, but still showing some damage. Vimentin-immunoreactivity is green; nestin-immunoreactivity is red; vimentin–nestin coexpression is yellow; and Hoescht nuclear label is blue; cc, central canal; scale line = 20 μm.

cies of urodeles, including larval stages, are needed to confirm this possibility.

NeuN is often used as a marker for mature neurons (e.g., Horner et al., 2000), although neither the definition of "mature" is always clearly defined nor the function of the NeuN protein is known. In the developing mammalian nervous system, NeuN is expressed in postmitotic neurons that are initiating cellular and morphological differentiation (Mullen et al., 1992). In the adult mammalian hippocampus, a few NeuN/BrdU positive cells can be found 1 day after BrdU injection, and this number increases considerably after 3 days (Kempermann, 2006). Similarly, we detected ependymal cells coexpressing BrdU-ir and NeuN-ir 1 day after BrdU injection in *P. cinereus*. These cells began to express NeuN even as they remained within the ependymal layer, although this expression was quite light.

In *P. cinereus*, there was a great deal of variation in the intensity and location of NeuN immunoreactivity and the size of nuclei expressing NeuN. Although anti-NeuN antibody primarily stains the nuclei of most neuronal cells types in the adult mouse brain and spinal cord, the cytoplasm can also be immunoreactive, although usually at a lower intensity (Mullen et al., 1992; Lind et al., 2005). By contrast, we found that the neuronal cytoplasm of processes in *P. cinereus* spinal cords, primarily in the undamaged more proximal spinal cord, can be intensely immunoreactive, outrivaling the intensity of nuclei in the same sections. In addition, the intensity of nuclear NeuN immunoreactivity in *P. cinereus* varied greatly within the same section, as did the size of nuclei. Because levels of NeuN expression vary in different cell types at different times in developing mice central nervous system, high levels of NeuN expression may correspond to the state of differentiation or level of cell activity (Mullen et al., 1992; Lind et al., 2005). Some evidence exists to support either of these hypotheses in that axonal injury strongly affects expression of NeuN in facial motor neurons, less so in spinal cord neurons (McPhail

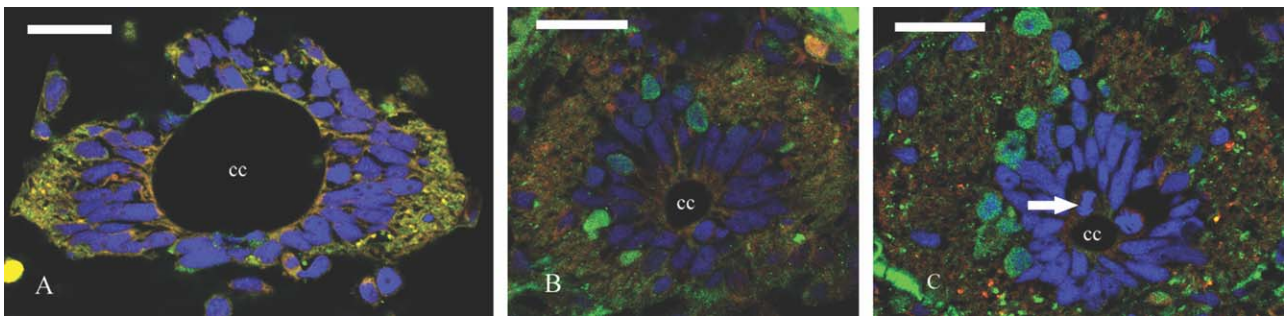

Fig. 11. Expression of nestin and vimentin in a spinal cord 14 days after autotomy. **A**: Distal section. **B** and **C**: Progressively more cranial sections. Vimentin-immunoreactivity is green; nestin-immunoreactivity is red; vimentin–nestin coexpression is yellow; and Hoescht nuclear label is blue; cc, central canal; white arrow points to a mitotically active cell in the ependymal layer; scale line = 40 μm.

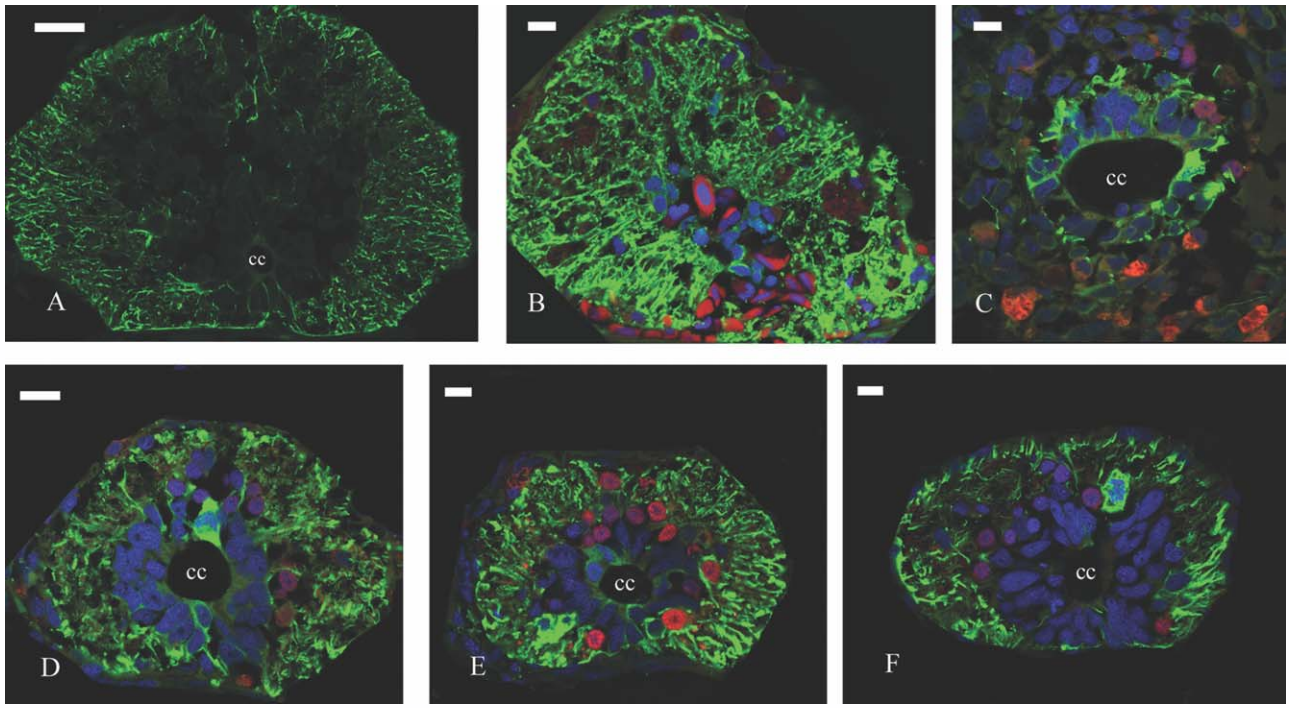

Fig. 12. GFAP expression in a normal spinal cord and in spinal cords after autotomy. **A**: Normal spinal cord. **B**: Caudal-most damaged spinal cord of a 5-day regenerating spinal cord. **C**: Growing ependymal tube in a 2-week regenerating spinal cord. **D**: A more cranial section in a 2-week regenerating spinal cord. **E** and **F**: A 3-week-old regenerating spinal cord showing peripheral GFAP expression. GFAP-immunoreactivity is green; NeuN-immunoreactivity is red; and Hoescht nuclear label is blue; cc, central canal; scale line = 20 μm.

et al., 2004). In the regenerating spinal cords in *P. cinereus*, the more uniform intensity of NeuN immunoreactivity in normal (unregenerating) spinal cords supports this suggestion as cells are not likely to be differentiating and more likely to be functioning similarly to one another.

Nestin/Vimentin Expression

In *P. cinereus*, vimentin was expressed 2–4 days before nestin in the perinuclear cytoplasm of the ependymal layer, although this could not be considered a growing ependymal tube; by 5 days and later, both nestin and vimentin were expressed by the perinuclear cytoplasm of the ependymal cells, whether considered ependymal layer or ependymal tube. Thus, it seems as if the damaged spinal cord quickly upregulates vimentin and probably nestin, even before there is an identifiable ependymal tube. Walder et al. (2003) reported that nestin and vimentin were upregulated in *P. waltl* and *N. viridescens* in the regenerating ependymal tube 1 week after tail amputation, reaching highest intensity at 2 weeks before decreasing and disappearing. In axolotls, vimentin immunoreactivity did not appear until 2–3-week postlesioning (O'Hara et al., 1992). Comparisons with these species and *P. cinereus* can only provisionally be made, as neither study examined nestin or vimentin expression before 1 week; that being said, *P. cinereus* seems to begin steps to spinal cord regeneration earlier than these nonautotomizing species. More proximally, in these early *P. cinereus*

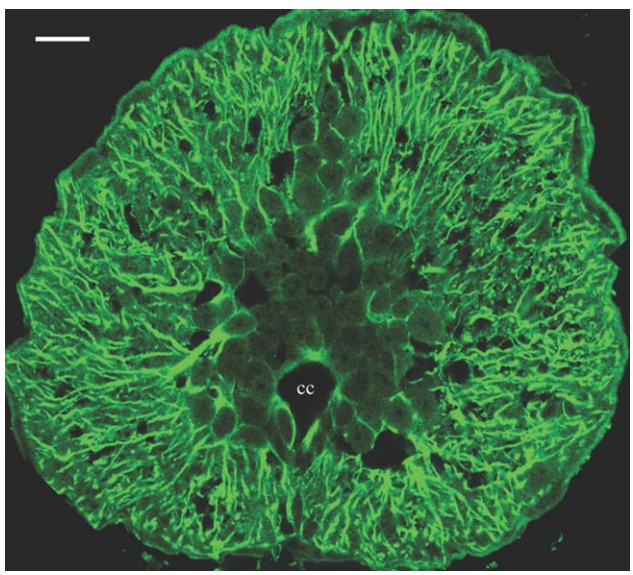

Fig. 13. GFAP expression in an intact, never regenerated, portion of a spinal cord 5 days after autotomy. GFAP-immunoreactivity is green; cc, central canal; scale line = 30 μm.

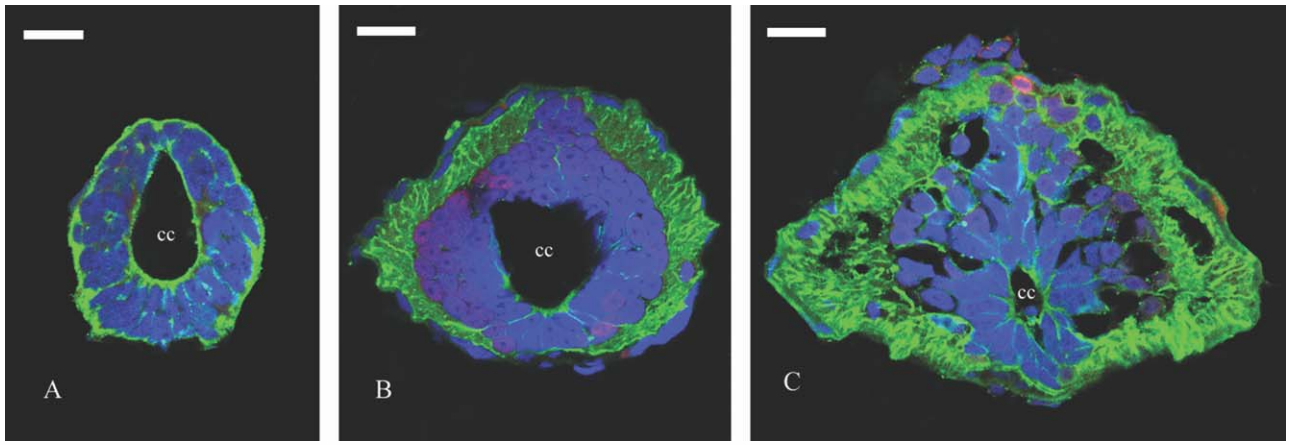

Fig. 14. GFAP immunoreactivity 66 days after autotomy. **A**: Distal section. **B** and **C**: Progressively more cranial sections. GFAP-immunoreactivity is green; NeuN-immunoreactivity is red; and Hoescht nuclear label is blue; cc, central canal; scale line = 30 μm.

regenerates (up to 14 days), both nestin and vimentin were expressed in processes of the white matter and associated with what looked like enlarged cells that may be migrating microglial cells. Nestin has been reported by at least one study to be expressed by microglia (Sotelo et al., 1994), as has vimentin (Graeber et al., 1988), and the shape and position of the large labeled cells in our sections are the same as we have seen in our lectin studies of *P. cinereus* microglia (unpublished observations). Surprisingly, it is hard to interpret the white matter processes that are immunoreactive for both nestin and vimentin as being radial. Further, this immunoreactivity was present in proximal sections in sections containing complete spinal cords, although vimentin was present for a longer period of time than nestin. Finally, vimentin immunoreactivity in more proximal sections was surprisingly intense in the perinuclear cytoplasm of cells peripheral to the ependymal layer, many of which must be neurons, based on NeuN-ir labeling, although we did not do double labeling experiments with NeuN and vimentin to confirm this. In mammals, vimentin is coexpressed with neurofilament proteins in young neurons, disappearing in mature neurons (Cochard and Paulin, 1984), except in the olfactory epithelium (Schwob et al., 1986). Because our control spinal cords showed little or no vimentin or nestin expression in neurons, these proteins must be upregulated in regenerating spinal cords, rather than continually expressed as Schwob et al. (1986) showed in olfactory receptor neurons. Further, vimentin and nestin are upregulated in the spinal cord cranial to the plane of amputation, not just in the regenerating ependymal tube, again suggesting that the intact spinal cord of regenerating salamanders also participates in the repopulating the growing spinal cord. Clear radial fibers were vimentin positive in more proximal, usually complete spinal cord sections. Although Walder et al. (2003) reported no significant vimentin in normal *P. waltl* spinal cords, Zamora and Mutin (1988) reported heavy labeling in perinuclear cytoplasm and radial arborizations of periependymal cells.

GFAP

In *P. cinereus*, as reported for other urodeles (Zamora and Mutin, 1988; Naujoks-Manteuffel and Roth, 1989; Holder et al., 1990; O'Hara et al., 1992; Arsanto et al., 1992; Lazzari et al., 1997; Walder et al., 2003), GFAP is expressed in radial processes in the white matter of the normal spinal cord, often clearly within the endfeet at the subpial surface. In addition, GFAP appeared to be perinuclear in some cells in the gray matter, which only some studies reported (Zamora and Mutin, 1988; Naujoks-Manteuffel and Roth, 1989; Lazzari et al., 1997), whereas others stated this never occurred (Holder et al., 1990; O'Hara et al., 1992). Rarely did studies of other urodeles report that soma in the ependymal layer are GFAP-positive (Walder et al., 2003). There are, however, differences in the reported position of radial glial cell bodies, with some studies placing the cell bodies in the layer immediately adjacent to the central canal (Walder et al., 2003), which is where BrdU-ir studies such as the one reported here for *P. cinereus* indicate they are, whereas other studies report that radial glial cell bodies are displaced into the periependymal gray matter (Zamora and Mutin, 1988; Naujoks-Manteuffel and Roth, 1989; Holder et al., 1990; Lazzari et al., 1997). Spinal cord regeneration in *P. cinereus* is marked by an increase in GFAP expression within processes and ependymal cell bodies, especially those undergoing mitosis. Further, this upregulation of GFAP

extends cranially within the damaged and regenerating spinal cord and into what appears to be normal spinal cord. Walder et al. (2003) also reported an increase in GFAP expression in the distal regenerating spinal cord, although they did not look in any detail in more cranial sections of the spinal cord; they reported that GFAP expression is the highest in the normal spinal cord and in the more undifferentiated (distal) regenerate within 1–2 weeks after amputation; thus, they conclude that GFAP expression is transiently lost just as nestin and vimentin are expressed. Others (Arsanto et al., 1992; O'Hara et al., 1992) only observed GFAP expression in processes and endfeet of regenerate, 2–4 weeks after amputation, respectively. In comparison, GFAP expression in regenerating *P. cinereus* seems to upregulate more rapidly and more extensively within the spinal cord cranial to the site of autotomy.

Known adult mammalian neurogenic zones (the subventricular zone (SVZ) of the lateral ventricles and the subgranular layer (SGL) of the hippocampal dentate gyrus) contain several cell types with specific GFAP, vimentin, and nestin expression patterns. GFAP-expressing astrocytes in these zones are the primary neuronal precursors (Doetsch et al., 1997; Seri et al., 2004); in the SVZ, these cells also express vimentin and nestin, whereas in the SGL, some of these precursors also express nestin (Seri et al., 2004). GFAP expression is then lost in the transiently amplifying progenitor cells after asymmetric division of the primary neuronal precursor cells, but nestin continues to be expressed. Eventually nestin expression also is lost, to be replaced by neuronal markers, such as NeuN. Thus, spinal cord regeneration in urodeles follows a similar pattern of expression of markers as for mammalian adult neurogenic zones, and the more complicated expression of nestin and vimentin in *P. cinereus* than what is reported by Walder et al. (2003) for *P. waltl* and *N. viridescens* calls into question whether or not the expression or re-expression of nestin and vimentin indicates a reversion of ependymal cells to a less mature phenotype, as they interpreted, as opposed to a generally more plastic spinal cord that is linked to the continual tail growth in urodeles. Vimentin and nestin expression in regenerating *P. cinereus* spinal cords is not only limited to the ependymal tube but also appears cranial to the plane of amputation and not just in the ependymal layer.

Summary

P. cinereus shows mitotic activity within the ependymal layer of the regenerating ependymal tube as well as more proximally in the spinal cord cranial to the plane of autotomy. This range of mitotic activity is more extensive than reported for other urodeles, which cannot autotomize their tails. NeuN expression appears in ependymal cells 1 day after BrdU injection, although this expression is light. NeuN expression in other cells is variable and often intense in both cell bodies and in processes. In addition, this species shows upregulation of nestin, vimentin, and GFAP within days after tail autotomy; further, this expression is upregulated cranially within the spinal cord cranial to the plane of autotomy, not just within the extending ependymal tube. Thus, the undamaged portion of the spinal cord is far more active in regeneration than has been reported in other urodeles.

ACKNOWLEDGMENTS

The authors thank Erin Vanselous, Rachel Margolis, Patrick Skelton, Kyle Davis, and Brenna Duffy for providing technical assistance.

LITERATURE CITED

Arsanto J-P, Komorowski TE, Dupin F, Caubit X, Diano M, Geraudie J, Carlson BM, Thouveny Y. 1992. Formation of the peripheral nervous system during tail regeneration in urodele amphibians: Ultrastructural and immunohistochemical studies of the origin of the cells. J Exp Zool 264:273–292.

Benraiss A, Arsanto JP, Coulon J, Thouveny Y. 1997. Neural crest-like cells originate from the spinal cord during tail regeneration in adult amphibian urodels. Dev Dyn 209:15–28.

Benraiss A, Arsanto JP, Coulon J, Thouveny Y. 1999. Neurogenesis during caudal spinal cord regeneration in adult newts. Dev Genes Evol 209:363–369.

Chernoff EAG, Stocum DL, Nye HLD, Cameron JA. 2003. Urodele spinal cord regeneration and related processes. Dev Dyn 226:295–307.

Cochard P and Paulin D. 1984. Initial expression of neurofilaments and vimentin in the central and peripheral nervous system of the mouse embryo in vivo. J Neurosci 4:2080–2094.

Dahl D. 1981. The vimentin-GFA protein transition in rat neuroglia cytoskeleton occurs at the time of myelination. J Neurosci Res 6:741–748.

Del Rio-Tsonis K, Tsonis PA. 2003. Eye regeneration at the molecular age. Dev Dyn 226:211–224.

Dinsmore C. 1977. Tail regeneration in the plethodontid salamander, *Plethodon cinereus*: Induced autotomy versus surgical amputation. J Exp Zool 199:163–176.

Doetsch F, Garcia-Vedugo JM, Alvarez-Buylla A. 1997. Cellular composition and three-dimensional organization of the subventricular germinal zone in the adult mammalian brain. J Neurosci 17:5046–5061.

Doetsch F, Caille I, Lim Da, Garcia-Verdugo JM, Alvarez-Buylla A. 1999. Subventricular zone astrocytes are neural stem cells in the adult mammalian brain. Cell 97:703–716.

Doyle K, Khan M, Cunningham AM. 2001. Expression of the intermediate filament protein nestin by sustentacular cells in mature olfactory neuroepithelium. J Comp Neurol 437:186–195.

Egar M, Sinder M. 1972. The role of ependyma in spinal cord regeneration in the urodele, *Triturus*. Exp Neurol 37:422–430.

Eng LF, Lee YL. 1995. Intermediate filaments in astrocytes. In: Kettermann H, Ranson DR, editors. Neuroglia. Oxford: Oxford University Press. pp 650–667.

Ferretti P, Zhang F, O'Neill P. 2003. Changes in spinal cord regeneration though phylogenesis and development: Lesions to be learnt. Dev Dyn 226:245–256.

Fredericksen K, McKay RDG. 1988. Proliferation and differentiation of rat neuroepithelial precursor cells in vivo. J Neurosci 8:1144–1151.

Fukuda S, Kato E, Tozuka Y, Yamguchi M, Miyamoto Y, Histasune T. 2003. Two distinct subpopulations of nestin-positive cells in adult mouse dentate gyrus. J Neurosci 23:9357–9366.

Graeber MB, Steit WJ, Kreutzberg GW. 1988. The microglial cytoskeleton: Vimentin is localized within activated cells *in situ*. J Neurocytol 17:573–580.

Hockfield S, McKay RDG. 1985. Identification of major cell classes in the developing mammalian nervous system. J Neurosci 5:3310–3328.

Holder N, Clarke JDW. 1988. Is a correlation between continuous neurogenesis and directed axon regeneration in vertebrate nervous system? Trends Neurosci 11:94–99.

Holder N, Clarke JDW, Kamalat T, Lane EB. 1990. Heterogeneity in spinal radial glia demonstrated by intermediate filament expression and HRP labeling. J Neurocytol 19:915–928.

Horner PJ, Power AE, Kempermann G, Kuhn HG, Palmer TD, Winkler J, Thal LJ, Gage FH. 2000. Proliferation and differentiation of progenitor cells throughout the intact adult rat spinal cord. J Neurosci 20:2218–2228.

Iten LE, Bryant SV. 1976. Stages of tail regeneration in the adult newt, *Nothophthalmus viridescens*. J Exp Zool 196:283–292.

Kempermann G. 2006. Adult Neurogenesis: Stem Cells and Neuronal Development in the Adult Brain. New York: Oxford University Press. 426 p.

Lazzari M, Franceschini V, Ciani F. 1997. Glial fibrillary acidic protein and vimentin in radial glial of *Ambystoma mexicanum* and *Triturus carnifex*: In immunocytochemical study. J Brain Res 38:187–194.

Lind D, Franken S, Kappler J, Jankowski J, Schilling K. 2005. Characterization of the neuronal marker NeuN as a multiply phosphorylated antigen with discrete subcellular localization. J Neurosci Res 79:295–302.

Mchedlishvili L, Epperlein HH, Telzerow A, Tanaka,EM. 2007. A clonal analysis of neural progenitors during axolotl spinal cord regeneration reveals evidence for both spatially restricted and multipotent progenitors. Development 134:2083–2093.

McPhail LT, McBride CB, McGraw J, Steeves JD, Tetzlaff W. 2004. Axotomy abolishes NeuN expression in facial but not rubrospinal neurons. Exp Neurol 185:182–190.

Mullen RJ, Buck CR, Smith AM. 1992. NeuN, a neuronal specific nuclear protein in vertebrates. Development 116:201–211.

Namiki J, Tator CH. 1999. Cell proliferation and nestin expression in the ependyma of the adult rat spinal cord after injury. J Neuropathol Exp Neurol 58:489–498.

Naujoks-Manteuffel C, Roth G. 1989. Astroglial cells in a salamander brain (*Salamandra salamandra*) as compared to mammals: A glial fibrillary acidic protein immunohistochemistry study. Brain Res 487:397–401.

Nye HLD, Cameron J, Chernoff EAG, Stocum DL. 2003. Regeneration of the urodele limb: A review. Dev Dyn 226:280–294.

O'Hara CM, Egar MW, Chernoff EAG. 1992. Reorganization of the ependyma during axolotl spinal cord regeneration: Changes in intermediate filament and fibronection expression. Dev Dyn 193:103–115.

Schwob JE, Farber NB, Gottlieb DI. 1986. Neurons of the olfactory epithelium in adult rats contain vimentin. J Neurosci 6:208–217.

Seri B, Garcia-Verdugo JM, McEwen BS, Alvarez-Buylla A. 2001. Astrocytes give rise to new neurons in the adult mammalian hippocampus. J Neurosci 21:7153–7160.

Seri B, Garcia-Verdugo JM, Collado-Morente L, McEwen BS, Alvarez-Buylla A. 2004. Cell types, lineage, and architecture of the germinal zone in the adult dentate gyrus. J Comp Neurol 478:359–378.

Shaw G, Osborn M, Weber K. 1981. An immunofluorescent microscopical study of the neurofilament triplet proteins, vimentin, and glial fibrillary acidic protein within the adult rat brain. Eur J Cell Biol 26:68–82.

Sotelo C, Alvarado-Mallart R-M, Frain M, Vernet M. 1994. Molecular plasticity of adult Bergmann fibers is associated with radial migration of grafted Purkinje cells. J Neurosci 14:124–133.

Tapscott SJ, Bennett GS, Toyama Y, Kleinbart F, Holtzer H. 1981. Intermediate filament proteins in the developing chick spinal cord. Dev Biol 86:40–54.

Tohyama T, Lee V-Y, Rorke LB, Marvin M, McKay RDG, Trojanowski JQ. 1992. Nestin expression in embryonic human neuroepithelium and in human neuroepithelial tumor cells. Lab Inves 66:303–313.

Wake DB, Dresner IG. 1967. Functional morphology and evolution of tail autotomy in salamanders. J Morph 122:265–306.

Walder S, Zhang F, Ferretti P. 2003. Up-regulation of neural stem cell markers suggests the occurrence of dedifferentiation in regenerating spinal cord. Dev Genes Evol 213:625–630.

Wiese C, Rolletschek A, Kania G, Blyszczuk P, Tarasov KV, Tarasova Y, Wersto RP, Boheler KR, Wobus AM. 2004. Nestin expression—A property of multi-lineage progenitor cells? Cell Mole Life Sci 61:2510–2522.

Zamora AJ, Mutin M. 1988. Vimentin and glial fibrillary acidic protein filaments in radial glia of the adult urodele spinal cord. Neuroscience 27:279–288.

Zhang F, Ferretti P, Clarke JDW. 2003. Recruitment of postmitotic neurons into the regenerating spinal cord of urodeles. Dev Dyn 226:341–348.